NUMERICAL ADVANCEMENTS IN JACKUP FOUNDATION SIMULATIONS

Erick Kencana and Okky Purwana*
Geo Oceanics (formerly National University of Singapore)

Hartono Wu
Singapore Institute of Technology

* *corresponding author: okky.purwana@geo-oceanics.com*

ABSTRACT

In recent years, advancements in large deformation finite element (LDFE) methods for tackling large deformation problems has made possible the simulations of continuous spudcan penetration that mimicking more realistic actual installation with evolving mechanisms. The numerical advancements have also enabled simulations of complex problems often encountered in jack-up operations such as spudcan-footprint interactions, spudcan-pipeline interactions, spudcan-pile interactions, spudcan extraction, etc. Such large deformation soil-structure interaction problems could not be adequately handled by the conventional small-strain or Lagrangian-based finite element analysis due to severe mesh distortion. Among available LDFE strategies, Couple Eulerian-Lagrangian (CEL) method is deemed a robust method in view of its effectiveness in overcoming the mesh distortion issue. In this paper, a continuous simulation of spudcan penetration, extraction and re-penetration at various offset distances on a multi-layered soil profile was performed to demonstrate the performance of CEL numerical technique and the selected soil constitutive models.

KEY WORDS: jack-up, spudcan, numerical modelling, large deformation finite element

1. INTRODUCTION

Large deformation finite element (LDFE) approach for simulations of jack-up spudcans has been more frequently adopted in practice for various problems associated with jack-up operations in the past decade. The use of such advanced numerical modelling techniques is normally intended to handle certain soil conditions or soil-structure interaction problems that are too complex for analytical or simplified calculations or even small-strain finite element (SSFE) approach. Routine assessments of jack-up foundations are usually performed using simplified or empirical procedures. However, for certain complex problems where the mechanics are not clearly understood or where analytical and empirical knowledge is limited, physical modelling (e.g., centrifuge experiments) or calibrated numerical simulations can be relied upon at least to assure reasonably conservative outcome. Rapid advancement of the numerical modellings in the past decade and its extensive calibrations against physical modelling demonstrates the constantly improving performance of LDFE techniques for realistic simulation of a complex soil-structure interaction problem.

Numerous studies on the numerical simulations of spudcan penetrations in multi-layered soils using LDFE approach have been published by many researchers, e.g., Hossain and Randolph [1], Tho et al. [2], Hu et al. [3] and Zheng et al. [4]. Tho et al. [5] and Chow et al. [6] modelled the effects of spudcan penetrations on adjacent piles. Hartono et al. [7], Zheng and Wang [8] and Jun et al. [9] performed the simulation of spudcan-footprint interactions in clays. Khoa et al. [10] presented a simulation of spudcan penetration and extraction to investigate soil movements at an adjacent pipeline location. In Tho et al. [11], an LDFE modelling strategy for spudcan penetration and re-penetration in a multi-layered soil was discussed. Zhang et al. [12] and Templeton [13] investigated the effect of installation on the bearing capacity of a spudcan under combined loading in non-homogeneous clays. This non-exhaustive list of studies showcases the maturity of the state-of-the-art finite element methods for a wide spectrum of spudcan assessments encompassing typical jack-up foundation problems encountered in practice either for hydrocarbon explorations or renewable energy.

This paper aims to demonstrate the applicability and advantages of LDFE technique as a readily practical assessment tool to simulate a complete process of a spudcan deployment in a multi-layered soil and to reveal the complex interactions between the spudcan and soil throughout the penetration-extraction evolution process. In the simulation, the spudcan was progressively advanced from the mudline level to the final penetration depth corresponding to a target preload footing reaction in a single analysis. Subsequently, the spudcan was fully extracted followed by a re-penetration at various offset distances onto the changing seabed topology created by the first spudcan installation. During the re-penetration, the spudcan load responses were monitored and the mechanism of spudcan-footprint interactions was investigated. At the final penetration depth upon the first installation, the foundation capacity envelope (yield surface) under combined loading was established taking into account the installation effect on the soil shear strength profile including the sand plug formation beneath the spudcan.

2. EVOLUTION OF NUMERICAL MODELLING TECHNIQUES FOR SPUDCAN PENETRATION

There are two distinct approaches of finite element method for simulating spudcan penetration, namely wished-in-place and pushed-in-place. The former was employed in earlier attempts of investigating spudcan penetration owing to rudimentary numerical approaches accessible at that time, e.g., Lagrangian approach or small-strain finite element. Several studies pointed out that this approach inherently ignores critical aspects for realistic prediction, such as the evolutions of pressure-dependent soil behavior, failure mechanism, and evolving seabed and sub-seabed geometries, i.e., resulting backflow, cavity depth, and soil plug when the spudcan approaches deeper penetration in layered soils.

For problems involving extremely large soil displacements such as spudcan penetration, the conventional small-strain or Lagrangian-based finite element analysis is inadequate due to severe mesh distortion. For problems involving large deformations that could not be handled by the same Lagrangian mesh, new mesh must be regenerated and the solution variables mapped from the original to the new mesh at a certain frequency during the analysis [2]. In recent years, advancement in LDFE methods for tackling large deformation problems has made possible continuous spudcan penetration simulations and more realistic mimicking of the actual installation. As discussed in detail in Tho et al. [2], LDFE analyses, in general, can be broadly categorized into three methods that employ different remeshing and variable solutions mapping strategies, namely, Rezoned meshes, Arbitrary Lagrangian-Eulerian (ALE) and Coupled Eulerian-Lagrangian (CEL).

The Remeshing and Interpolating Technique with Small Strain (RITSS) developed by Hu and Randolph [14] is an example of the rezoned meshes technique. In this strategy, the new mesh can have a different configuration from the original mesh and the mapping is performed through an interpolation technique. Implementation of such a technique however requires elaborated user subroutines that are not readily available in commercial software.

In ALE method, a new mesh is created during the analysis similar to the rezoned mesh technique but the mesh must maintain the same elements and connectivity as the original mesh as the frame of reference. In other words, the re-meshing is performed by repositioning the nodes and no new element is created nor deleted during the process. The mapping is carried out through an advection process. While the remeshing strategy can somewhat overcome the potential severe localized mesh distortion issue in a Lagrangian analysis, this method can lead to a premature termination for spudcan penetration simulation involving soil backflow. This method cannot handle a deep penetration problem in layered soils [15].

Coupled Eulerian-Lagrangian (CEL) finite element approach is considered a robust LDFE method for modelling spudcan installation and interaction with any adjacent structures. In Eulerian analysis, the spatial position of the nodes is fixed and thus the mesh undergoes zero distortion during the analysis. Instead, the materials can move (flow) from one element to another which circumvent the problem associated with severe mesh distortion in the case of Lagrangian analysis. In addition to tackling the mesh distortion issue and simulating very large deformations, the CEL method can also be paired with advanced constitutive soil models to produce more realistic spudcan penetration responses.

In CEL modelling, spatial migration of soil state parameters due soil flow must be incorporated for

realistic simulation of soil responses. This is especially important for non-homogeneous soil and layered soil profiles. Lacking of these considerations may result in unrealistic physical soil response and spudcan penetration behaviour. Without material tracking, the undrained shear strength profile remains identical to that of the initial state despite the large soil deformation during the spudcan penetration process. The migration of soil material of different shear strength due to the plastic flow mechanism is clearly evident when material tracking is implemented. Tho et al. [16] discussed in detail the effect of material tracking on the shear strength distribution and the bearing response of a penetrating spudcan in non-homogenous clay.

3. SOIL CONSTITUTIVE MODELS

Advanced soil constitutive models such as modified Mohr-Coulomb or hypoplastic for sands and Tresca with strain-softening for clays are generally adopted in CEL modelling for spudcans. Tresca model is a sub-class of the conventional Mohr-coulomb model with zero friction angle and zero dilatancy angle. The Tresca model is often used in total stress analysis to simulate soil failure conditions. To simulate clay soil exhibiting a strain-softening behavior, the conventional Tresca model needs to be further modified by reducing its yield surface size to capture the strain-softening behavior. Although the modification is explicit at the beginning of every time step and it depends on an accumulated plastic strain, the model has been proven suitable for simulating the strain-softening behavior [17].

Similar approach to the Tresca with strain-softening model, Hu et al. [18] modified the Mohr-Coulomb model to simulate sand behavior exhibiting strain-hardening and post-peak softening. The evolution of strain hardening and softening in the modified Mohr-Coulomb depends on an empirical accumulated plastic strain. The key advantage of the modified Mohr-Coulomb model is the simplicity in application. The model however does not regulate the deformation behavior nor enable an evolution of stress-strain relationship that can simulate the change of sand packing density, which typically encountered in large deformation problems. From numerous validations against centrifuge tests in sand over clay profiles, however, the model is deemed able to simulate the spudcan penetration responses reasonably well.

A more advanced critical-state framework model, sand hypoplastic originally developed by Herle and Gudehus [19] is also available for CEL. Unlike the modified Mohr-Coulomb, the changes in strength behavior are mathematically made consistent with deformation behavior which is coupled with the void ratio of the sand. Owing to the critical-state framework, the model only needs a set of parameters to simulate the wet-side and dry-side behaviors in triaxial tests unlike the modified Mohr-Coulomb which needs multiple sets of parameters. The sand hypoplastic model is more suitable to describe the stress-dependent soil deformation behavior around a penetrating spudcan when complex stress paths due to backflow and the formation of sand-plug are of concern. The use of the sand hypoplastic model for spudcan penetration has been demonstrated in Qiu and Grabe [20] and Bienen et al. [21].

4. CASE STUDY

In this paper, a continuous simulation of spudcan penetration, extraction and re-penetration at various offset distances on a multi-layered soil profile was performed to demonstrate the performance of CEL numerical technique and the selected soil constitutive models. At the final penetration depth corresponding to an assumed preload footing reaction, yield surfaces in VH (vertical-horizontal) and VM (vertical-moment) load spaces were established accounting for the post-installation effect. For simplicity, the spudcan is only allowed to move vertically and restrained in lateral and rotational directions. Although in reality the spudcan can slide and rotate due to the flexibility of the leg and the global stiffness of the jack-up, this simplified approach is expected to produce conservative spudcan reaction forces. An example of full modelling of jack-up and spudcan footprint interaction is discussed in Jun et al. [9].

A rectangular spudcan measuring 9.0m wide x 14.0m long with a preload bearing pressure of approximately 700 kPa was selected representing an offshore wind turbine installation jack-up. The selected hypothetical soil profile consists of a top very dense sand layer (D_R = 85%) of 6m thick overlying a 12m thick firm clay layer and underlain by a thick strong soil stratum. Such a soil profile is often encountered in offshore wind farms and is considered more realistic than assuming a significantly thick

clay layer. The underlying clay layer has a shear strength profile of 45 kPa at the sand-clay interface and increasing linearly with depth at a gradient of 1.5 kPa/m. For the purpose of demonstrating CEL performance, the third layer is simplified as a rigid bottom to increase the computational efficiency assuming negligible effects on the load-displacement response of the spudcan.

4.1 Numerical Modelling

The CEL simulation was performed in Abaqus [22]. The horizontal boundary of the soil domain is fixed at 2.75 times the spudcan width measured from the spudcan edge. This clearance is deemed to be sufficiently large to minimise the boundary effects while allowing an optimum computational time. The bottom boundary of the soil domain is set at a depth of 18m from the mudline representing the bottom strong soil layer. A relatively coarse mesh size, approximately 0.05 times the spudcan width, is used within 0.75 times the spudcan diameter from the symmetry axis to cover significant soil movements induced by the spudcan penetration. Although a finer mesh of approximately 0.02B should be used [16], a consistent trend of spudcan responses can still be achieved with the medium coarse mesh despite the tendency for slight overprediction of the spudcan resistance. For saving computation time and taking advantage of the symmetrical shape of the spudcan, only half of the domain is included in the model as shown in Figure 1. Zero flow velocity is prescribed normal to this plane of symmetry. The half domain allows the simulation of spudcan vertical movements (penetration and extraction) as well as swipe and probe tests for the determination of the foundation capacity envelope.

The soil domain consists of 8-noded Eulerian brick elements denoted as EC3D8R of approximately 150,000 in size. A void layer was defined above the mudline to allow the soil to heave. The sand layer was simulated using sand hypoplastic model (Herle and Gudehus, [19]) while the underlying clay was modeled with strain-softening Tresca model (Einav and Randolph, [23]). The same properties of sand used in Qiu and Grabe [18] was adopted. The undrained shear strength was allowed to reduce to one-third of the initial definition due to strain softening behavior depending on the accumulated plastic shear strain. A ratio of E_u/s_u of 150 is assumed for the clay layer while the Poisson's ratio is set to be 0.30 and 0.495 for sand and clay respectively. The finite element mesh is shown in Figure 1.

For enhanced computational efficiency, the spudcan was modelled as a rigid shell part instead of using solid deformable brick elements which is computationally more time consuming. The spudcan was modelled with approximately 3,000 discrete rigid Lagrangian R3D4 elements. The interface between the spudcan and soil was modelled using surface-to-surface contact formulation to formulate the normal and tangential behaviours. The hard contact pressure-overclosure relationship was adopted for the normal behaviour with zero-penetration conditions but allowed separation after contact. The basic isotropic Coulomb friction model is adopted for the tangential behaviour formulated based on the penalty method.

In order to achieve a balance between matching a quasi-static state as closely as possible and at the same time reducing the computational time, the spudcan was set to continuously penetrate into the seabed through the application of a prescribed velocity of 0.2 m/s. At this rate of spudcan penetration, the inertial effect is deemed to be negligible.

5. SIMULATION RESULTS OF SPUDCAN LOAD-DISPLACEMENT RESPONSE

5.1 Spudcan Penetration and Extraction

At the preload footing reaction considered, the spudcan pushes through the sand layer forming a sand plug below the spudcan post-peak resistance. After punch through, the spudcan tip advances to approximately 10m depth with the composite foundation, consisting of the spudcan and sand plug, fully embedded inside the underlying clay layer. In Figure 2, the numerically simulated spudcan load-displacement response is presented for both penetration and extraction stages. At the final penetration depth of approximately 10m, a squeezing mechanism is observed below the composite foundation around which a localized plastic flow takes place. Upon extraction, given the cohesionless nature of the soil surrounding the spudcan, the soil uplift resistance is mainly contributed by the soil weight and shear resistance within the partially-filled cavity above the spudcan. There is no bottom resistance registered and the spudcan was immediately separated from the sand plug upon extraction.

The change in soil profile and seabed topology are shown in Figure 3. At the post-installation stage, it is evident that the strength profile of the underlying clay surrounding the composite foundation is different from the original linearly increasing profile. The sand plug measures approximately 0.9 times the initial sand layer thickness. After the full spudcan extraction from 10m depth, a pile of sand filling the cavity and a depression is formed at a slope similar to the repose angle of the sand. The simulation results also display a more realistic footprint condition with laterally variable sand void ratios and the corresponding relative densities as illustrated in Figure 4. Around the depression area, the sand packing density changes from the originally very dense (D_R = 85%) to loose sand ($D_R \approx$ 30%) while slightly denser sand ($D_R \approx$ 90%) than the original is observed at the top portion of the sand plug left in the footprint. These results demonstrate the importance of material tracking and the selection of appropriate constitutive models in CEL modelling. It also demonstrates the realistic formation of sand plug beneath penetrating spudcan and the corresponding load-penetration responses associated with this mechanism in multi-layer soil profile.

5.2 Spudcan Re-penetration and Interaction with Footprints

At this stage, the spudcan re-penetrates into the footprint simulating a location revisit or a re-positioning using the same jack-up but at an offset distance from the center of the first installation. Three offset distances (center-to-center) were modelled in the simulation, i.e., 0.25B, 0.50B and 0.75B where B is the width of the spudcan. Besides the asymmetrical seabed surface at re-penetration trajectory, the re-penetration of the spudcan involves complex soil states created by the first installation. In addition, the lateral variation in the seabed topology and the properties of the subsurface soils also induce horizontal and moment loads acting at the spudcan. Although numerous spudcan-footprint interaction studies have been performed in clay soils, it was unclear whether the findings could be extrapolated to sand over clay profiles.

The spudcan load responses at the various offset distances are plotted in Figure 5 and the mechanisms are shown in Figure 6. For the same applied preload footing reaction as in the first penetration, the final spudcan penetration depth changes, i.e., approximately 6.6m, 12.0m and 14.6m (measured from the original mudline) for 0.25B, 0.50B, and 0.75B offset distance respectively. At 0.25B offset, the re-penetrated spudcan stops at shallower depth compared to the first installation. This is due to the spudcan re-penetrated into the significant proportion of the existing sand plug already existed from the first installation.

As the offset distance becomes larger, the re-penetration depth for the same target preload is found to go deeper. At 0.75B offset, the re-penetration depth of 14.6m is significantly deeper than the first installation despite that the load-penetration curve resembles that of the first installation with the same sand plug formation that breaks away from the first installation. This deeper re-penetration is due to the variation in the undrained shear strength profile that is partially remoulded due to first installation. This phenomenon would have been rather complex to be anticipated with analytical assessment or engineering judgement.

The maximum horizontal load acting on the spudcan increases when the offset distance varied from 0.25B to 0.75B. This behaviour is consistent with the findings on spudcan-footprint interaction on clayey soil [9]. It is interesting to note that the spudcan responds differently in terms of moment load. The maximum moment load appears to produce somewhat unique patterns at different offset distances and was found to increase at larger penetration depths for certain offset distances such as at 0.25B re-penetration. Depending on the water depth at a jacking location, spudcan moment load may be the bigger contributor (than spudcan horizontal load) to the resulting total moment load at the leg-hull connection level.

As described in Figure 6, the re-penetration forms an asymmetrical sand plug which in turn lead to non-uniform bearing pressures at the spudcan bottom despite the full bottom-contact being achieved at the final penetration depth. For the 0.25B and 0.50B offset distances, the new sand plug combines with the old sand plug left by the first installation at the respective final penetration depth. At 0.25B offset distance, the induced moment is more severe at greater re-penetration depths due to the spudcan predominantly re-penetrated into the existing sand plug while at the same time interacting with the underlying clay layer. On the other hand, due to the relatively large separation distance at 0.75B offset, the new sand plug

"breaks" away from the old one as the spudcan penetrates deeper. This may explain the reason for diminishing horizontal and moment loads at large penetration depths for the 0.75B offset distance.

The numerical simulations provide insight into the complex soil state and spudcan responses during re-penetration which could have been overlooked if a simplistic assumption of laterally uniform soil properties were made or if the reported general trends observed from a single clay layer case were adopted.

6. FOUNDATION CAPACITY UNDER COMBINED LOADING

6.1 Foundation capacity in non-homogeneous soil profiles

In the case of soil profile and the soil states at the final spudcan penetration depth simulated herein, uncertainties arise as to how the foundation yield surface should be determined. The available framework recommended in ISO 19905-1 is most applicable for relatively homogeneous sands or clays. Given the spudcan rests on the sand plug pushed into the underlying clay, the determination of a reasonably conservative foundation yield surface is non-trivial as a closed-form expression for such a situation is currently not available. From a centrifuge experiment of spudcan capacity after punch-through, Hu et al. [25] reveals a considerably higher uniaxial horizontal capacity and a similar moment capacity in comparison with that for a single clay layer.

For spudcan embedded in clay overlying sand layer, Wang et al. [26] has investigated the effects of the underlying sand layer on the combined failure envelope. In the study, small-strain finite element analyses were performed with a pre-embedded spudcan in the clay layer. Liu et al. [27] evaluated the foundation capacity envelope of a spudcan wished-in-place on the surface of sand overlying clay layer, i.e., preloading footing reaction lower than the punch through resistance. Despite the similarity of soil profiles to that considered in the present study, the findings are not applicable for post-punch-through situations. Therefore, a preliminary investigation of the foundation yield surface was undertaken in the present study to demonstrate the reliability of the numerical method used in the present study.

6.2 Validation of numerical model

The numerical framework used for developing the foundation capacity was first validated against relevant studies in the public domain. Estimation of combined bearing capacity of a deeply embedded spudcan in normally consolidated soft clay using LDFE approach has been reported by Zhang et al. [12]. In Zhang [28], the corresponding centrifuge tests results were also reported. In the former study, a continuous spudcan penetration was simulated using remeshing and interpolation technique using small strain (RITSS) method. The effect of clay sensitivity on the post-installation soil strength profile and the corresponding size of yield surface was also investigated.

In the present study, the same spudcan and soil profile [12, 28] were adopted for validating combined bearing capacity envelopes of the spudcan. The installation effect at the target final penetration depth was modeled using CEL. The resulting soil profiles were then mapped onto a Lagrangian model and the spudcan capacity under combined loading was subsequently calculated using SSFE analyses. This strategy allows the consideration of installation effects while ensuring optimum computation of the foundation capacity. Zhang et al. [28] discussed that relatively small displacement is required for mobilizing ultimate capacity of the spudcan and therefore small-strain finite element approach is expected to provide reasonable predictions. This is also shown in the validation exercise that the foundation capacity estimated from LDFE is consistent with that from SSFE.

Both swipe test and probe test were undertaken to validate VM and HM envelopes respectively as discussed in Zhang et al. [12]. In the swipe test, the spudcan was first displacement-controlled until the target penetration depth is achieved and followed by rotation to develop VM surface while the spudcan penetration depth is held constant. On the other hand, in probe test a proportion of the ultimate vertical load is initially applied as a direct force and maintained while fixed displacement ratio probes are prescribed to establish the failure envelope in HM plane.

For modelling the installation effect, the material tracking and strain softening functions were activated in CEL resulting in the change in the soil strength profiles surrounding the spudcan during penetration. The comparison of post-installation soil profiles and the foundation yield surface in VM (H = 0) and HM ($V/V_0 = 0.5$) load spaces are presented Figure 7. The CEL model predicts somewhat smaller VM and HM capacity than the numerical modelling results reported in Zhang et al. [12]. The numerically simulated VM and HM yield surfaces however are in closer agreement with the centrifuge tests results [28]. This validation demonstrates the numerical framework adopted in the present study has a consistent performance with the published studies which have been calibrated against physical modelling.

6.3 Simulation and results

The same CEL approach as that used in the validation case was applied to the hypothetical multi-layered soil profile assumed in the present study as discussed in Section 4. In the present simulation, the size of the yield surface in VM plane (H = 0) was investigated by swipe test. Any change in the moment capacity of the spudcan in the multi-layered soil profile, in comparison with that in homogeneous soil, is expected to directly influence the spudcan rotational fixity upon storm loading. For the swipe test, only load path commencing from the maximum vertical load (applied preload footing reaction) was simulated for comparison with the centrifuge tests results reported by Hu et al. [25].

The numerical simulated normalized load paths of the swipe test in the VM load space (H = 0) are plotted in Figure 8. The corresponding range of load paths derived from the centrifuge tests reported by Hu et al. [25] are also shown for comparison. From the comparison, it can be noted that the numerically simulated foundation envelope produces a consistent shape of the foundation envelope with that observed from the centrifuge tests. A significant increase in the moment capacity was found from the numerical model. For the multi-layered soil profile considered in the simulation, the normalized moment capacity, m_0 (peak in VM plane with H = 0) was found to be approximately 1.8 – 2.0 times the capacity in a single clay or sand layer. In addition to the contribution of the sand plug below the spudcan that forms a composite foundation, the increase in the combined foundation capacity can also be attributed to the proximity of the composite foundation bottom to the top of the strong soil stratum. Besides minimizing the uncertainties with regards to the influence of sand plug on the spudcan foundation capacity, reduced conservatism can be obtained through the validated numerical simulations.

7. SUMMARY

A continuous simulation of a spudcan deployment in a sand over clay profile has been performed using Coupled Eulerian Lagrangian (CEL) finite element technique combined with the state-of-the-art soil constitutive models. Such simulations of extremely large deformation problem were previously challenging, if not impossible, to be performed using the conventional Lagrangian-based small-strain analysis or Arbitrary Lagrangian-Eulerian (ALE) approach. The present study demonstrates the feasibility of the presently available numerical technique for realistic simulations of spudcan foundation installation in multi-layered soils or complex seabed topology. With the availability of more robust numerical techniques and soil constitutive models, potentially complex interactions between a spudcan and seabed can be identified from which more effective engineering solutions can be derived for mitigating spudcan installation risks. Numerical simulations can also be considered for cases beyond the range of applicability of the existing industry guidelines or those involving marginal utilizations of a jack-up capacity.

8. ACKNOWLEDGEMENTS

Part of this study was performed when the authors were associated with Centre for Offshore Research and Engineering (CORE) at the National University of Singapore. The authors gratefully acknowledge Emeritus Professor Chow Yean Khow and Emeritus Professor Leung Chun Fai for their support and guidance.

9. REFERENCES

[1] Hossain, M.S. and Randolph, M.F. (2010). "Deep-penetrating spudcan foundations on layered clays: numerical analysis", Geotechnique 60, No. 3, 171–184.

[2] Tho, K.K., Leung, C.F., Chow, Y.K. and Swaddiwudhipong, S. (2012). "Eulerian finite element technique for analysis of jack-up spudcan penetration", Int. J. Geomech., 12(1): 64-73.

[3] Hu, P., Stanier, S.A., Cassidy, M.J. and Wang, D. (2014). "Predicting peak resistance of spudcan penetrating sand overlying clay", J. Geotech Geoenviron Eng 140(2): 04013009.

[4] Zheng, J., Hossain, M.S. and Wang, D. (2017). "Numerical investigation of spudcan penetration in multi-layer deposits with interbedded sand layers", Géotechnique 67, No. 12, 1050–1066.

[5] Tho, K.K., Leung, C.F., Chow, Y.K. and Swaddiwudhipong, S. (2013). "Eulerian finite element simulation of spudcan-pile interaction", Canadian Geotechnical Journal, 50(6).

[6] Chow, Y.K., Kencana, E.Y., Leung, C.F. and Purwana, O.A. "Spudcan-pile interaction in thick soft clay and soft clay overlying sand: A simplified numerical solution", Applied Ocean Research, Volume 112, 102684.

[7] Hartono, Tho, K.K., Leung, C.F. and Chow, Y.K. (2014). "Centrifuge and numerical modelling of reaming as mitigation measure for spudcan-footprint interaction", Proceed. 2014 Offshore Technology Conference Asia, Kuala Lumpur, OTC-24835-MS.

[8] Zheng, J. and Wang, D. (2019). "Numerical investigation of spudcan-footprint interaction in non-uniform clays", Ocean Engineering 188, 106295.

[9] Jun, M.J., Kim, Y.H., Hossain, M.S., Cassidy, M.J., Hue, Y. and Park, S.G. (2020). "Numerical analysis of reinstallation of spudcans near footprints formed during prior installations", Applied Ocean Research 100, 102163.

[10] Khoa, D.V.H., Meyer, V.M. and Pike, R.J. (2020). "Case study: Spudcan-pipeline interaction at the Maria field - Challenges of data interpretation and comparison of predicted and measured soil deformation", 4th Int. Symp. on Frontiers in Offshore Geotechnics, Austin Texas, USA.

[11] Tho, K.K., Chan, N., Zhou, Y., Liu, J. and Zhou, S. (2015). "Case study of spudcan re-penetration using large deformation finite element approach", Jack-up Conference, City University, London.

[12] Zhang, Y., Wang, D., Cassidy, M. J. and Bienen, B. (2014). "Effect of installation on the bearing capacity of a spudcan under combined loading in soft clay." J. Geotech. Geoenviron. Eng. 140 (7): 04014029.

[13] Templeton III, J.S. (2021). "Eulerian Analysis of Jack-up Spud Can Foundation Performance", Jackup Conference, City University, London.

[14] Hu, Y., and Randolph, M. F. (1998). "A practical numerical approach for large deformation problems in soil." Int. J. Numer. Anal. Methods Geomech., 22(5), 327–350.

[15] Khoa, D.V.H. and Jostad, H.P. (2016). "Application of Coupled Eulerian-Lagrangian method for large deformation analyses of offshore foundations and suction anchors", Int. J. of Offshore and Polar Eng., Vol. 26, No. 3, pp. 304–314

[16] Tho, K.K., Leung, C.F., Chow, Y.K. and Swaddiwudhipong, S. (2011). "Important Considerations in the Application of Eulerian Technique for Spudcan Penetration Analysis". 13th Jack-up Conference, City University, London.

[17] Hossain, M. S. and Randolph, M. F. (2009). "Effect of strain rate and strain softening on the penetration resistance of spudcan foundations on clay", International Journal of Geomechanics, 9(3), 122-132.

[18] Hu, P., Wang, D., Cassidy, M.J. and Stanier, S.A. (2015). "Assessing the punch-through hazard of a spudcan on sand overlying clay", Géotechnique 65, No. 11, 883–896.

[19] Herle, I. and Gudehus, G. (1999). "Determination of parameters of a hypoplastic constitutive model from properties of grain assemblies". Mechanics of Cohesive-frictional Materials: An International Journal on Experiments, Modelling and Computation of Materials and Structures, 4(5), 461-486.

[20] Qiu, G. and Grabe, J. (2012). "Numerical investigation of bearing capacity due to spudcan penetration in sand overlying clay", Canadian. Geotech. J. 49, pp. 1393–1407.

[21] Bienen, B., Qiu, G. and Pucker, T. (2015). "CPT correlation developed from numerical analysis to predict jack-up foundation penetration into sand overlying clay", Ocean Engineering, 108, 216-226.

[22] Dassault Systemes. Abaqus 2022

[23] Einav, I. and Randolph, M. F. (2005). "Combining upper bound and strain path methods for evaluating penetration resistance". Int. J. Numer. Methods Engng 63, No. 14, 1991–2016.

[24] Mollaibrahimoglu, C., Sharp, L., van Tongeren, A., Hill, A.R. and Purwana, O.A. (2023). "Improving Performance of Spudcan Predictions during Installation", Jack-up Conference, City University, London.

[25] Hu, P., Bienen, B. and Cassidy, M.J. (2017). "Combined loading capacity of a spudcan in clay after penetrating through a sand layer", Géotechnique Letters 7, 97–103.

[26] Wang, Y., Cassidy, M.J. and Bienen, B. (2020). "Numerical Investigation of Bearing Capacity of Spudcan Foundations in Clay Overlying Sand under Combined Loading", J. of Geotech. and Geoenviron. Eng. 146(11): 04020117-1.

[27] Liu, Y., Zheng, J., Wang, D. and Liu, K. (2022). "Capacity of spudcan foundation on dense sand overlying clay under combined loading", Ocean Engineering 266 (2022) 112980.

[28] Zhang, Y. (2013). "A force resultant model for spudcan foundations in soft clay", PhD Thesis, University of Western Australia.

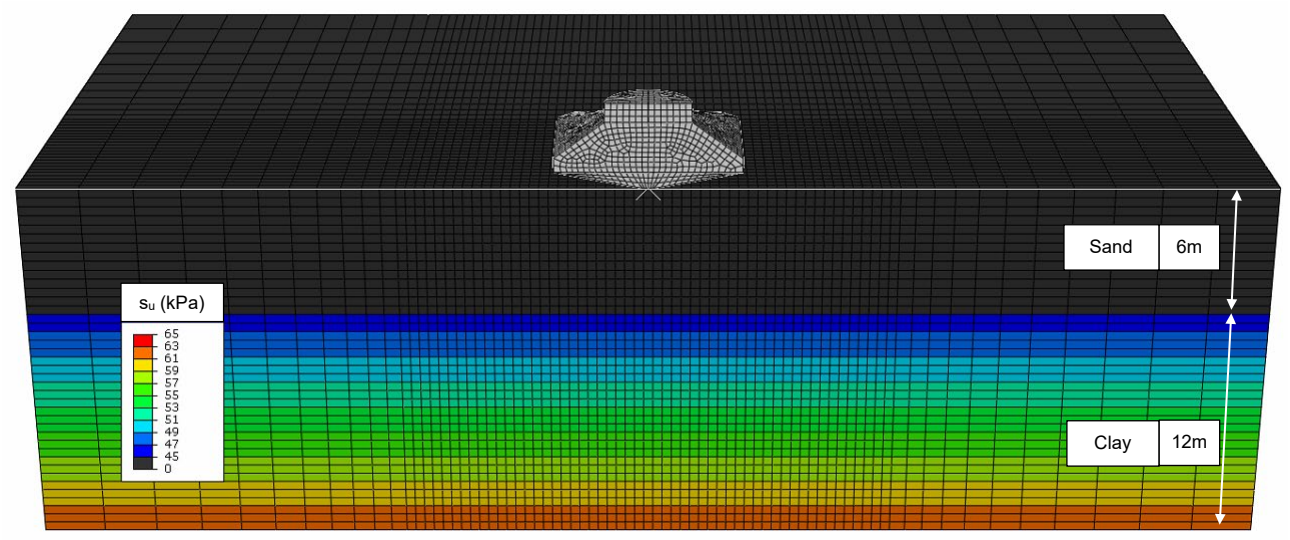

Figure 1 Finite element model used in present simulations (medium coarse mesh)

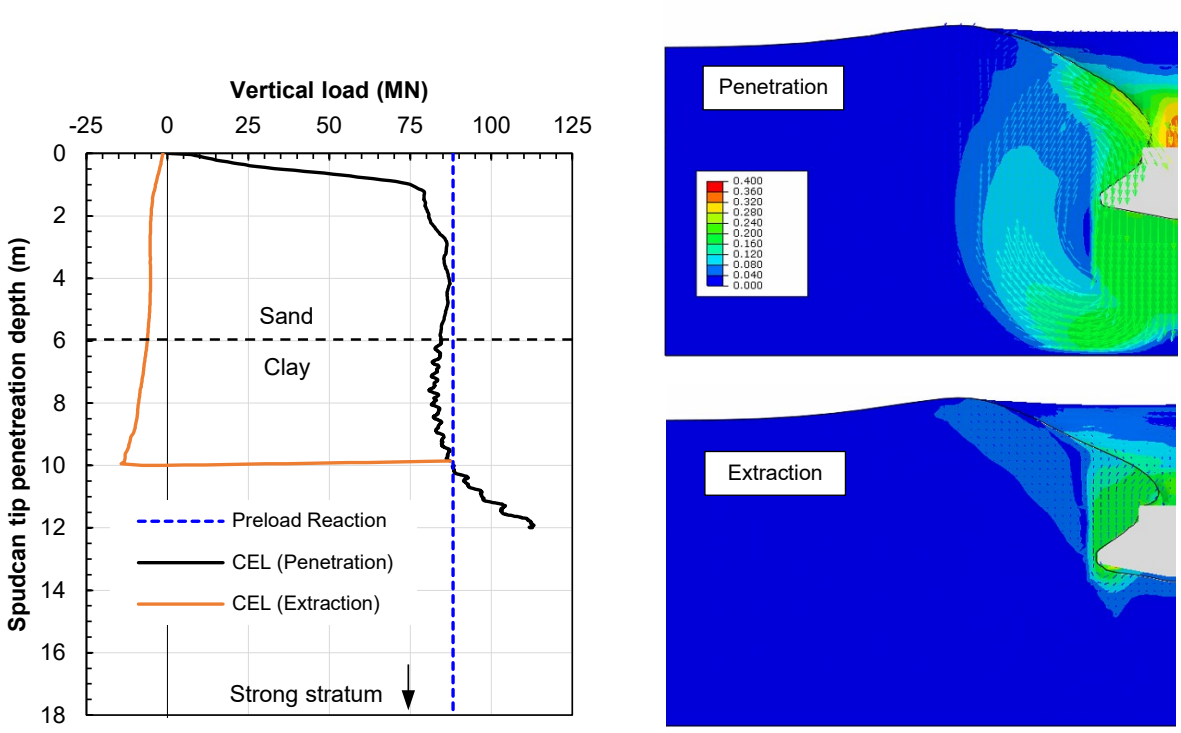

Figure 2 Spudcan load-displacement responses and soil movement patterns

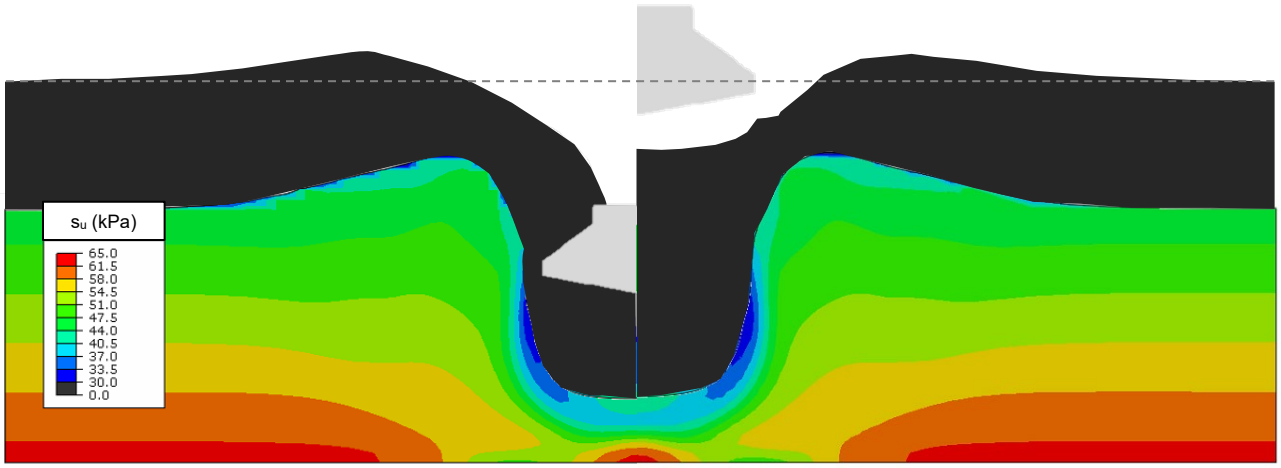

Figure 3 Soil profiles post-installation and changing seabed topology after spudcan extraction

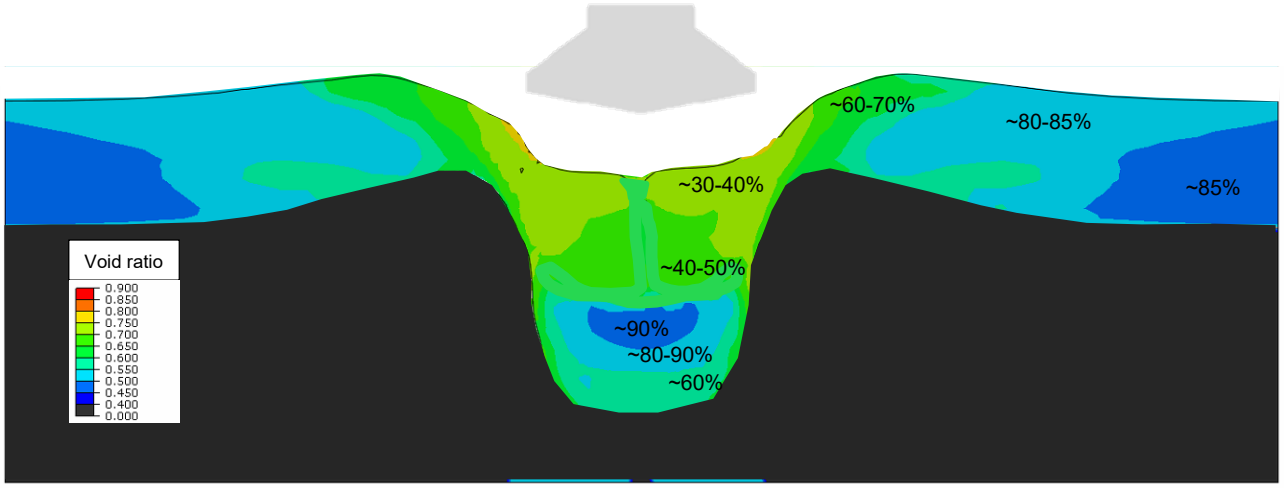

Figure 4 Post-installation void ratio in top sand layer and corresponding nominal relative density

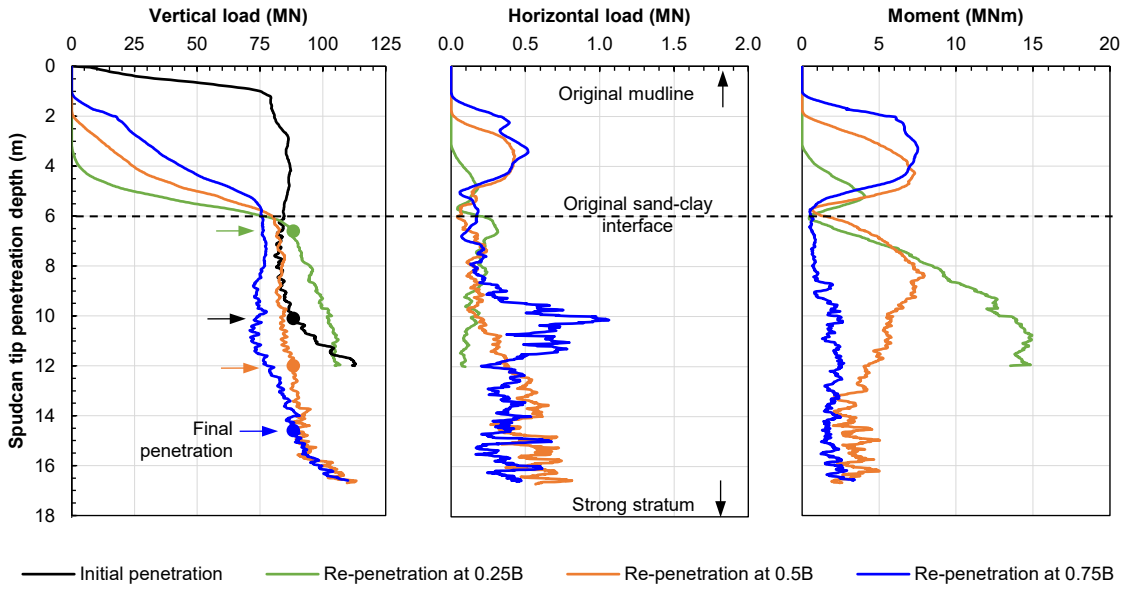

Figure 5 Spudcan load-displacement responses during spudcan re-penetration at various offset distances

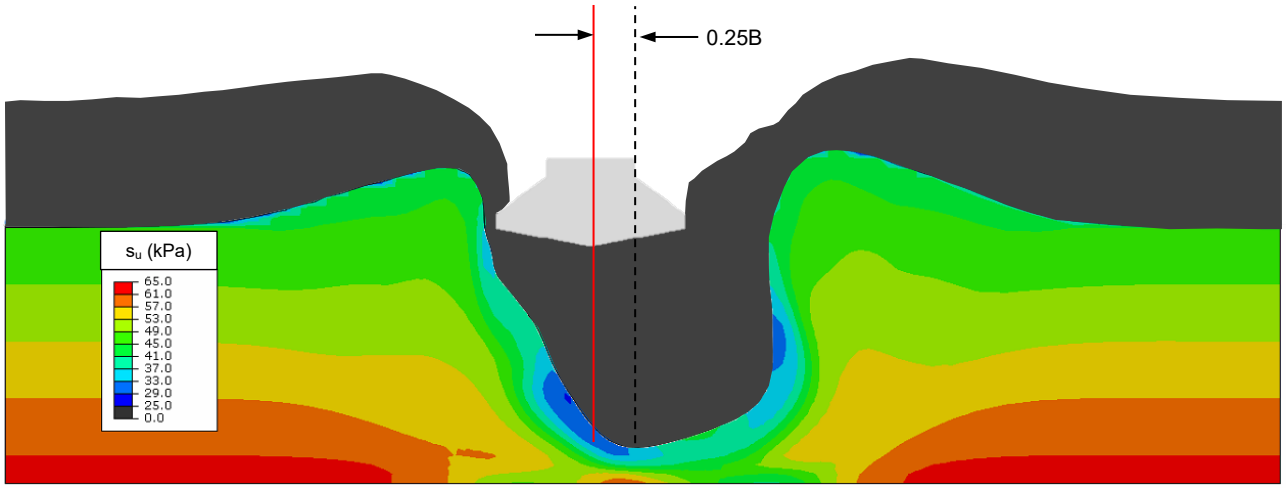

0.25B offset distance (6.6m final penetration depth)

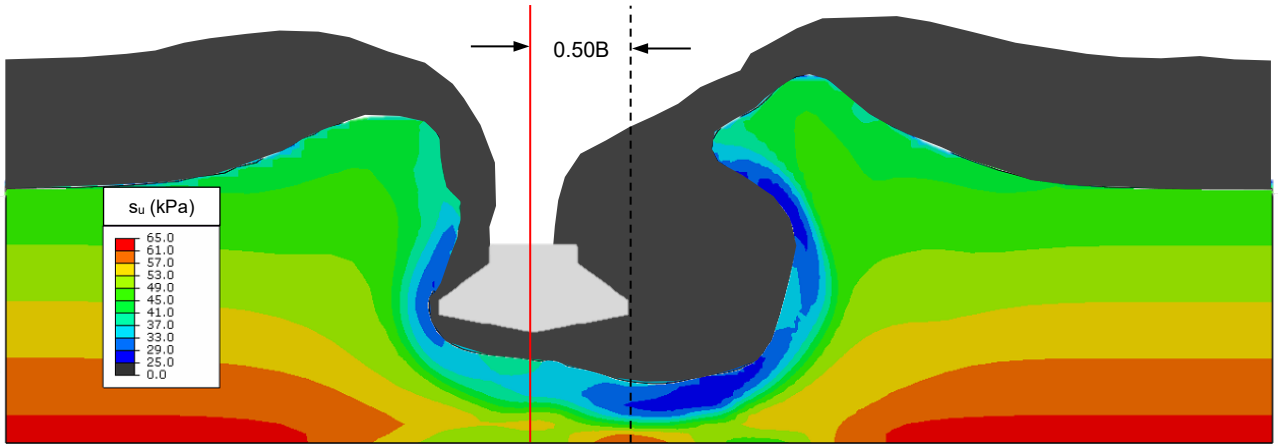

0.5B offset distance (12.0m final penetration depth)

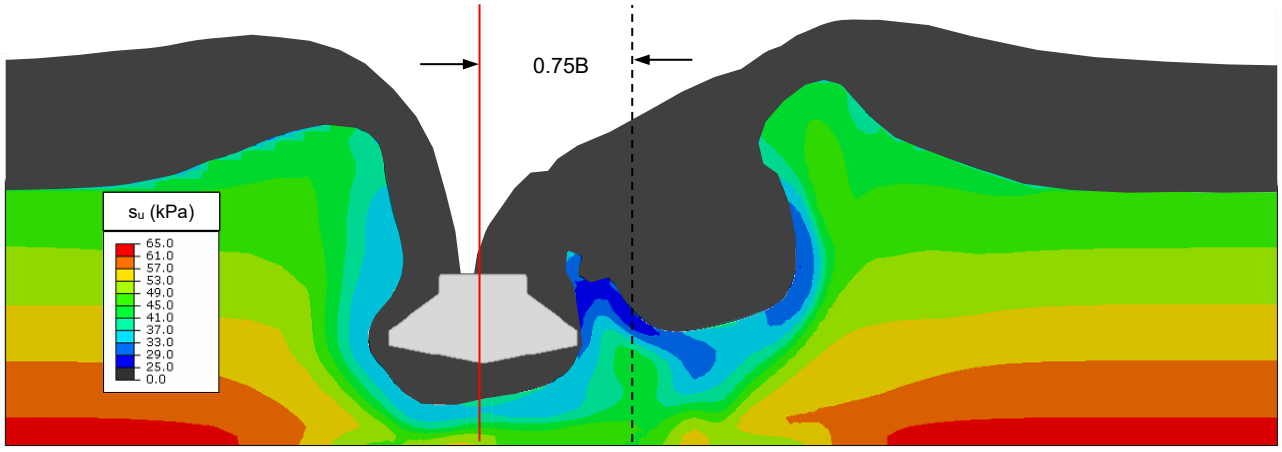

0.75 offset distance (14.6m final penetration depth)

Figure 6 Soil profiles after spudcan re-penetration at various offset distances

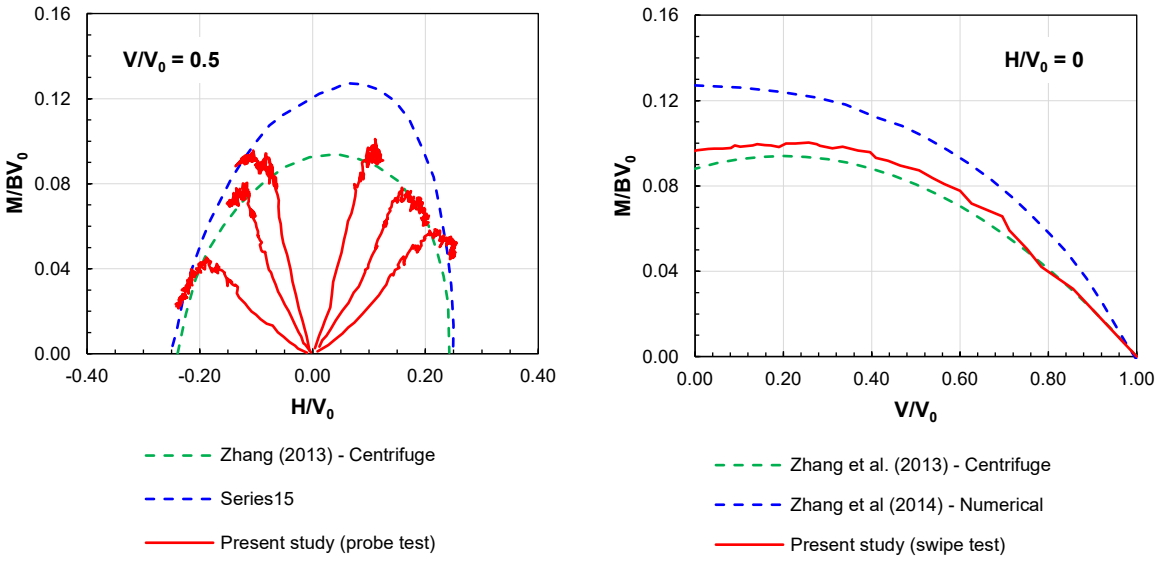

Figure 7 Validation of numerical framework for deeply embedded spudcan foundation capacity in normally consolidated clay

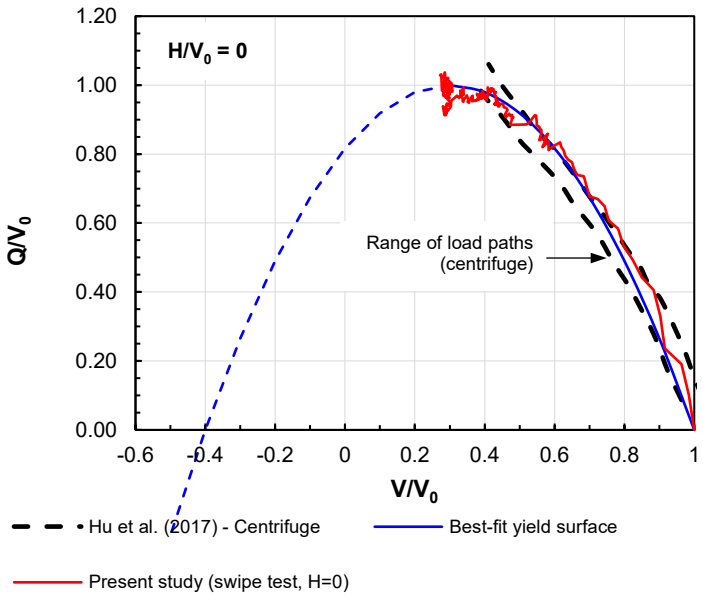

Figure 8 Numerically simulated spudcan foundation VM (H=0) capacity in sand over clay